Determining Large Scale Sandbar Evolution

Donald G. Bailey and Roger D. Shand

Image Analysis Unit, and Geography Department
Massey University, Palmerston North
Ph: +64 6 350 4063, Fax: +64 6 354 0207
E-mail: D.G.Bailey@massey.ac.nz

Abstract

To study the morphology of coastal sandbars and their change with time, it is necessary to obtain a sequence of bathymetric maps over the period of interest. Traditional techniques such as vertical aerial photography or echosounding over a grid are expensive and subject to environmental constraints, especially in higher energy situations. Photographic methods assume that the position and intensity of waves breaking on bars are strongly related to the position and depth of the bars. An alternative approach is to use image processing to transform a panorama of photographs taken from adjacent elevated ground.

The individual photographs are normalised with respect to lighting variations, and rectified to map coordinates using the horizon and two ground control points. However, the coordinates of interest are longshore and offshore distances. A smooth curve is therefore fitted through the shore baseline, and the image warped to make this line straight. The sandbar crest positions within in this image are detected, and then tracked with time to investigate how the bars evolve.

1. Background

A significant and increasing proportion of the worlds population and wealth is concentrated in the sand-dominated coastal zone [1]. This region, however, is highly variable and unstable with erosion exceeding deposition globally [2,3]. The predicted greenhouse associated sea-level rise is likely to exacerbate this situation [4,5]. There is clearly a practical need to maximise our understanding of the Earth's coastal systems.

The coastal zone can be subdivided into a number of interrelated subzones or subsystems, each characterised by distinctive processes and morphologies (see figure 1). Contemporary geomorphological field studies have tended to concentrate on the inner nearshore and backshore zones of low to moderate energy coasts [6], because of their relative ease of access.

To facilitate comprehensive nearshore investigations, in particular those on moderate to high energy coasts, methods of acquiring morphological data at a variety of scales, both spatial (10^1 to 10^{3+} metres longshore) and temporal (10^0 to 10^3days), are required.

2. Existing methods of bathymetric sampling

A variety of techniques have been used for bathymetric sampling and a summary is given in table 1. Ideally accurate 3-dimensional data is required for morphodynamic modelling. However, cost, longshore coverage limitations, and logistical problems prohibit the

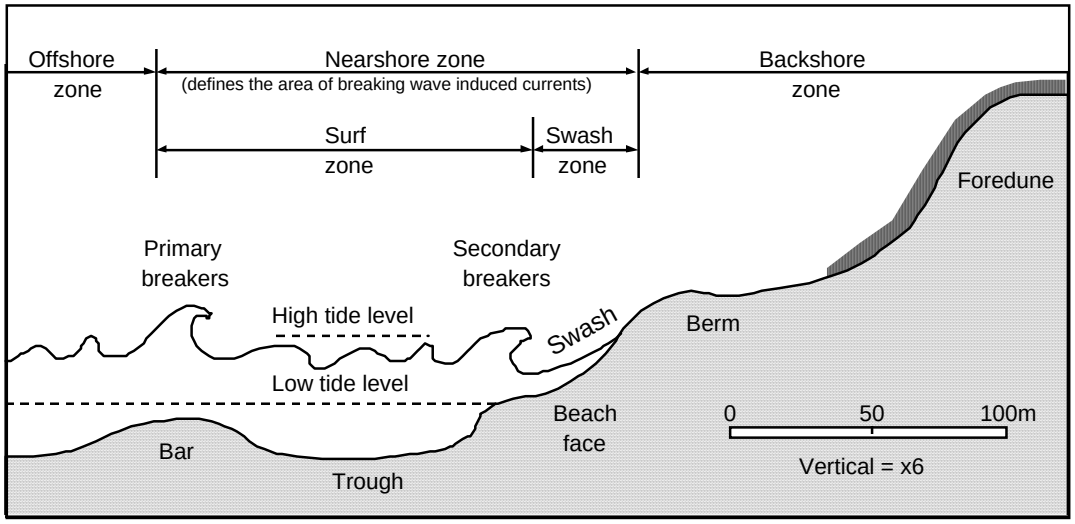

Figure 1: Profile depiction of typical (marine driven) coastal morphodynamic zones.

widespread use of the most definitive methods (A and B) especially in higher energy environments.

Imaging techniques (C and D) increase longshore coverage and utilise increased energy levels in the form of the breaking wave pattern and intensity to signal form and relative depth [7]. Atmospheric restrictions (cloudless conditions) and high costs restrict the aerial (including satellite) option.

A recent development has been elevated terrestrial imaging (C) incorporating rectification of the oblique pictures to map coordinates (vertical projection), and long-exposure techniques to improve morphological feature definition. This cheap and flexible method has great potential especially for the higher energy sand-dominated environments which also tend to be backed by elevated ground [8] suitable for camera sites.

Technique	Description	Environment for regular sampling	Coverage per day	Cost per day	Accuracy 3-D
A. Bottom moving instruments	Longshore transits. Offshore distances by EDM or cable. Depths by EDM or pressure transducer	Low/mod energy	Low	High	High
B. Surface moving instruments	Longshore transits. Offshore distances by sextant or EDM. Depths by echosounder	Low/mod energy	Low	High	High
C. Elevated terrestrial imaging	Oblique photo/video. Time exposure option. Location by grid overlay or rectification. Depth inferred from wave intensity	Mod/high energy	High	Low	Location high, depth mod
D. Aerial imaging	Vertical photographs. Location by reference points or rectification. Depth by waves or visible forms	Low/mod/ high energy	High	High	Location high, depth mod

Table 1: Nearshore morphological sampling: main methods and characteristics.

2.1 The rectified long exposure method

The initial work in developing this approach can be credited to Rob Holman and Tom Lippmann at Oregon State University. They utilised a 40 m tower and the extensive

resources of the US Army Corps of Engineers CERC Field Research Facility on the Outer Banks of North Carolina to refine and ground truth-test the technique (see [7] and [9]).

Their work, however, was based on the use of a single longshore image covering a rectified length of up to 660 m. Their images were taken at the same time each day regardless of atmospheric, sea or tide conditions, all of which greatly affect image quality and bathymetric representativeness.

It is necessary to explore the limits and possibilities of the method with respect to the morphological scale objectives described above. This paper covers our image processing work while the other aspects, that is the influences of equipment and environmental variations, are reported elsewhere [10].

3. Objectives

A panorama of eight photographs was taken from a single site 100 m behind and 43 m above the spring high tide mark. The four central shots were taken using a 55 mm focal length lens to give good coverage of the area without sacrificing detail. To obtain satisfactory resolution for the four end shots, a 135 mm focal length lens was used. Each photograph was taken using a three minute time exposure to average the effects of individual waves. The following image processing steps were carried out to maximise the resolution potential and to facilitate statistical analysis:

- Compensate for variations in image density.
- Enhance images such that 3-dimensional detail and longshore coverage is maximised.
- Correct for perspective distortion, including automatically calculating the horizon location and camera tilt.
- Straighten the coastline while minimising shore-normal distortion.
- Detect shore-parallel intensity maximums corresponding to the bars.

4. Image preprocessing

A 512 x 512 image is captured of each photograph, with a 2:3 aspect ratio. While capturing the photographs, it is ensured that the top and bottom edges of the photographs are visible in the image since these are required for determining the camera tilt. It is also ensured that the left and right edges of the photographs are out of the field of view, otherwise artefacts may be introduced when mosaicing the photographs.

Since the panorama spans about 160° there is a considerable variation in lighting from one photograph to another because of differing sun angles. In addition to this, there may be sun glare from the sea or clouds and vignetting caused by the lens and neutral density filters. These effects are all exacerbated by reciprocity failure caused by the long exposures required. The first step is to normalise the contrast range of each image as much as possible. This contrast normalisation is performed using the following steps:

1. The image is filtered by selecting the minimum pixel value within a 21 x 21 pixel box. This effectively shrinks the lighter regions of the bars preventing them from being removed by the process. At this stage we are interested in finding the background level.
2. This image is then filtered using the average pixel value within a 55 x 55 pixel box to obtain an estimate of the local average density. Variations in this image correspond to density variations in the original image.
3. The average is subtracted from the original image to remove the density variations. An offset of 128 is added to allow negative differences to be represented conveniently.

Figure 2: A typical image after normalising variations in lighting and enhancing the contrast.

4. Finally, the contrast of the image is enhanced using a linear stretch to expand the range of pixel values from 116 to 208 to fill the available range (0 to 255).

The resulting contrast normalised image is shown in figure 2.

5. Rectification

Each photograph has perspective distortion resulting from the viewing geometry. This distortion must be removed before the individual photographs can be mosaiced to give the full panorama. Finally, since the coast is curved, the image needs to be warped further to put the information into a form that is convenient to use.

5.1 Correction of perspective distortion

The first step in this process is to correct for the perspective distortion present in each of the images. At this stage, a convenient coordinate system is based on map coordinates. We have actually used rotated map coordinates since the stretch of coast under study runs SE to NW, resulting in unnecessarily large images to contain the detail of interest.

If we assume that the earth is flat (a reasonable assumption since the ranges of interest are within 3.5 km from the camera location) the perspective correction equation may be represented by

$$X = \frac{a_0 x + a_1 y + a_2}{a_6 x + a_7 y + a_8}, \quad Y = \frac{a_3 x + a_4 y + a_5}{a_6 x + a_7 y + a_8} \qquad (1)$$

where (x,y) are the pixel coordinates in the image before rectification, and (X,Y) are the corresponding rectified coordinates. Note that this equation will only correctly transform one 2-D plane to a second 2-D plane. The input plane is the film plane of the camera, and the output plane corresponds to sea level. The 9 unknowns in equation (1) are solved by knowing the camera position, the positions of two surveyed ground control points (GCPs) within each image, the sea level, and the horizon. The common denominator of the perspective transformation represents the perspective vanishing line in the photographs.

$$a_6 x + a_7 y + a_8 = 0 \qquad (2)$$

If the earth were truly flat, this line would correspond to the horizon. However, because of the curvature of the earth, the apparent horizon will be below the true "flat earth" horizon (figure 3). It can be shown that the angle between the true and apparent horizon is

$$\theta \approx \sqrt{\frac{2h}{R}} \tag{3}$$

where h is the height of the camera above sea level, and R is the radius of the earth. Although this angle is small ($\theta = 0.21°$ for h =43 m), the error is significant, giving a 4 pixel shift in the horizon for photographs taken using a 55 mm lens and a 9.5 pixel shift with a 135 mm lens.

From the positions of the ground control points in the image, the position of the apparent horizon is estimated. A linear edge detection operation is applied within that region to detect the maximum intensity gradient (corresponding to the horizon). A least squares fit is applied to the detected points to give the line of the horizon. This is then corrected for θ to give a_6, a_7 and a_8. Note that equation (2) is normalised so that

$$a_6^2 + a_7^2 = 1 \tag{4}$$

The program draws the detected horizon on the input image and asks the user if it has been detected correctly. If not, the user defines the correct horizon by entering two points. This step is necessary because the position of the horizon may not be detected accurately if the weather is hazy or if the sea has rough and calm patches on it.

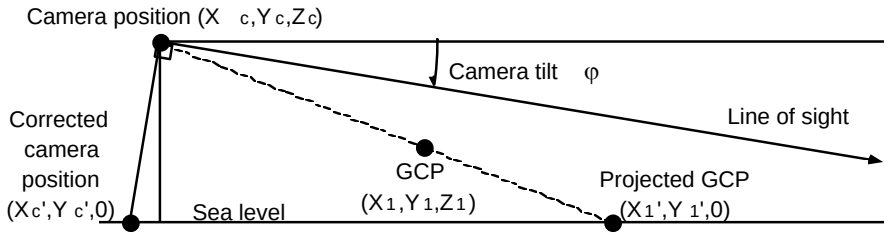

Figure 4: Correcting for camera tilt and projecting ground control points to sea level.

The next step is to reference the camera and ground control points to sea level (the reference plane for our perspective corrected image). The GCPs are projected to sea level as shown in figure 4. This projection may be represented as in equation (5).

$$X_1' = \frac{Z_1 X_c - Z_c X_1}{Z_1 - Z_c}, \quad Y_1' = \frac{Z_1 Y_c - Z_c Y_1}{Z_1 - Z_c} \tag{5}$$

Lines perpendicular to the horizon on the input image all fall on planes which pass through the camera. Therefore these lines all converge at the camera point in the rectified image. If the camera is tilted below the true horizon, the point of intersection of the horizon perpendiculars will move behind the camera as shown in figure 4. It is assumed that the pixel mid way between the top and bottom edge of the photograph is along the line of sight of the camera (that is normal to the film plane). The tilt is calculated knowing the angle of the line

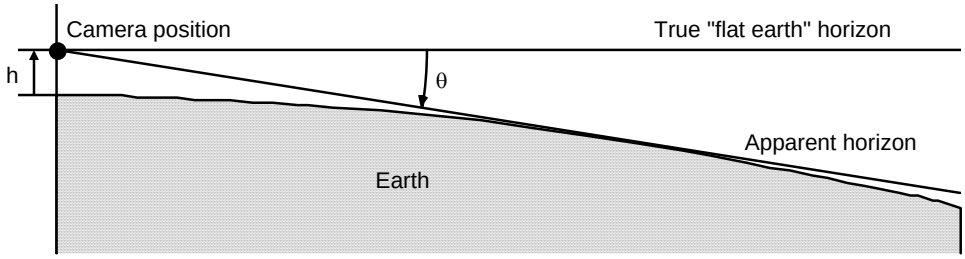

Figure 3: Error between true horizon and apparent horizon.

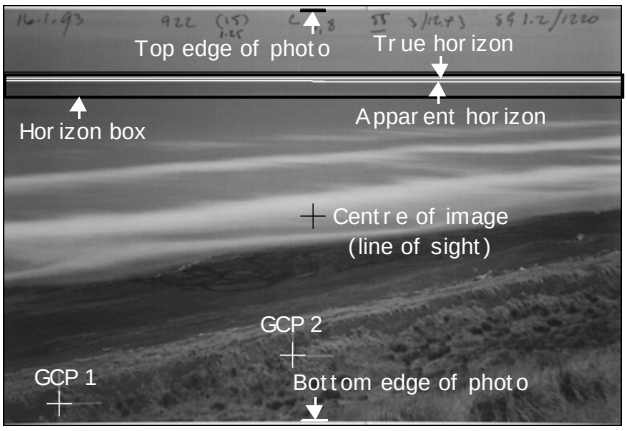

Figure 5: The input image with key features labelled.

of sight below the true horizon. The camera position may be referenced to sea level as

$$X_c^{'} = X_c - Z_c \tan\varphi \sin\gamma, \quad Y_c^{'} = Y_c - Z_c \tan\varphi \cos\gamma \tag{6}$$

where γ is the direction of the line of sight. In practise, the direction of the line of sight is calculated by solving equation (1) assuming no tilt (using (X_c,Y_c)). The centre pixel of the image (256,256) is then transformed to give the direction of the line of sight. This is used to correct the camera position for tilt and equation (1) is solved again. Figure 5 shows the input image with the key features labelled.

Lines perpendicular to the horizon intersect at the corrected camera position after transformation. These lines may be parameterised by

$$x = a_6 t + b_0, \quad y = a_7 t + b_1 \tag{7}$$

where b_0 and b_1 are arbitrary constants. Substituting these into equation (1) gives

$$\begin{aligned} X_c^{'} &= \underset{t\to\infty}{Limit} \frac{a_0(a_6 t + b_0) + a_1(a_7 t + b_1) + a_2}{a_6(a_6 t + b_0) + a_7(a_7 t + b_1) + a_8} \\ &= \frac{a_0 a_6 + a_1 a_7}{a_6^{\,2} + a_7^{\,2}} \quad = a_0 a_6 + a_1 a_7 \end{aligned} \tag{8}$$

Each GCP gives a further independent equation in a_0, a_1 and a_2, as in equation (9).

$$\begin{aligned} X_1^{'} &= \frac{a_0 x_1 + a_1 y_1 + a_2}{a_6 x_1 + a_7 y_1 + a_8} \\ &= \frac{a_0 x_1 + a_1 y_1 + a_2}{H_1} \end{aligned} \tag{9}$$

where H_1 is a constant (all its terms are known). Equation (8) and equation (9) for each GCP give three simultaneous equations that are solved to give

$$\begin{aligned} a_0 &= \frac{X_c^{'}(y_1 - y_2) - a_7(H_1 X_1^{'} - H_2 X_2^{'})}{a_6(y_1 - y_2) - a_7(x_1 - x_2)} \\ a_1 &= \frac{a_6(H_1 X_1^{'} - H_2 X_2^{'}) - X_c^{'}(x_1 - x_2)}{a_6(y_1 - y_2) - a_7(x_1 - x_2)} \\ a_2 &= X_1^{'} H_1 - a_0 x_1 - a_1 y_1 \end{aligned} \tag{10}$$

Similar equations may be obtained for a_3, a_4 and a_5. Equation (1) is then used to transform each pixel in the input image, giving figure 6. The transformed image is sampled with 2 m resolution.

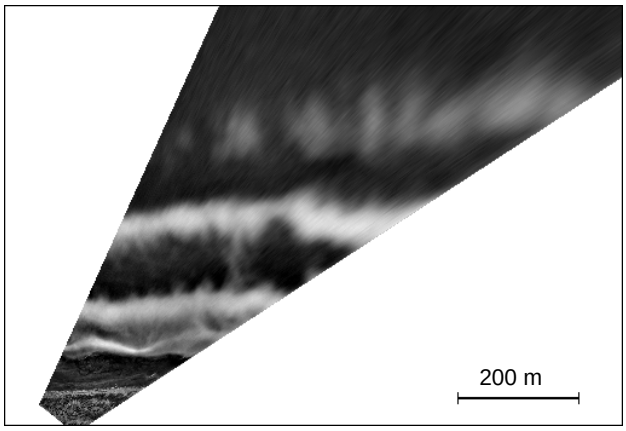

Figure 6: The perspective corrected image.

5.2 Mosaicing

After correcting for perspective distortions in each of the eight input photographs, the images are combined into a single view of the coast. The views provided by the individual photographs overlap slightly. To reduce the possibility of artefacts from the joins, in the region of overlap between adjacent views, the images are merged using a linear spline as shown in figure 7. The resulting mosaic is shown in figure 8.

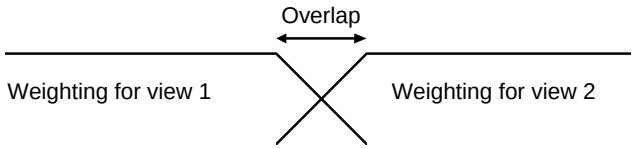

Figure 7: Linear spline applied to the overlap between images.

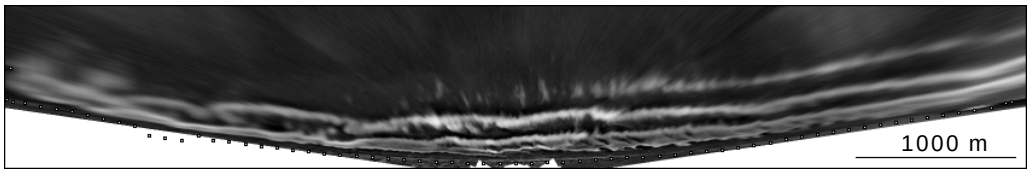

Figure 8: Mosaic of eight perspective corrected images.

5.3 Straightening of coastline

In determining the positions of the bars, a more useful coordinate system is longshore and offshore coordinates. To facilitate conversion to these coordinates, a separate series of ground control points was surveyed along the toe of the foredune at 100m intervals. These points define the baseline for offshore distance measurements. A smooth curve is fitted to these points using a piecewise parabolic fit. A least squares parabolic fit is made over 1000 m sections, with 500 m overlap between the sections. The overlapping regions are combined using a linear spline.

The image is then incrementally rotated (or unrolled) to make the baseline straight. At each point along the baseline, the shore normal is calculated and the image resampled along the shore normal. The resulting image is shown in figure 9. Having the offshore and longshore variations separated enables the offshore scale to be amplified to highlight the sandbar morphology.

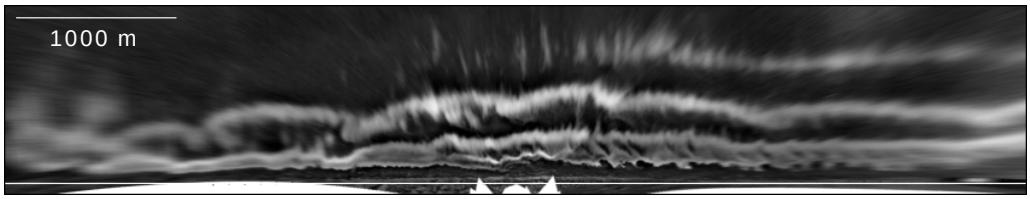

Figure 9: Image after straightening the coastline (offshore distance scale x2).

6. Detection of sandbars

The next step is to detect the positions of the sandbars. The positions of the bar crests can be inferred from the position of maximum intensity along the bar. Although not completely accurate (since the position of maximum intensity depends on both the tide and wave energy) this measure provides the best estimate from the information available. The bar crests are detected using the following steps:

1. The image is filtered by selecting the maximum pixel within a 1 x 21 pixel box. This is then subtracted from the image before filtering. The difference will be 0 only in the positions of local maxima, where local is defined by the 1 x 21 box. By thresholding the difference to select only the 0 pixels, the positions of all the local maxima are detected in the image.
2. Many of the local maxima detected correspond to noise, so the image is ANDed with the original to obtain the maximum values. This is then thresholded at an intensity of 80 to select only the significant maxima, corresponding to the bar crests.
3. Finally the detected crests are thinned to a single pixel thickness. The resulting image is shown in figure 10 overlaid on the original.

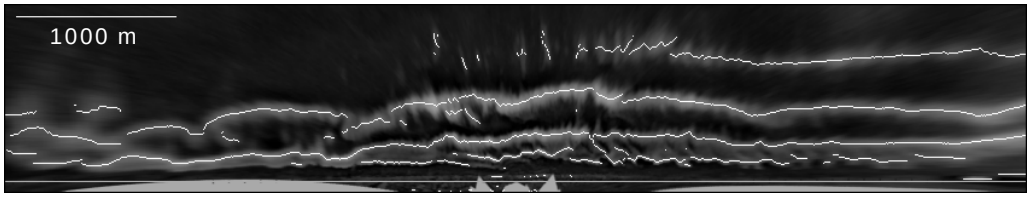

Figure 10: Detected sandbars (offshore distance scale x2).

Quantitative measurements may be made of the bar positions by measuring the offshore distances of the bars from the baseline. By examining a series of images taken at regular intervals, the morphodynamics of the coastal system may be investigated.

7. Summary

An inexpensive method of obtaining data for studying the time evolution of sandbars on moderate to high energy coasts is to use elevated terrestrial imaging. A panoramic series of eight oblique photographs are normalised with respect to lighting variations and rectified to map coordinates. The resulting mosaiced image is warped again, straightening the coastline, to give the more useful longshore and offshore coordinates. The positions of the bar crests are detected by the locating intensity maxima, and then tracked with time to study how the bars behave.

8. Acknowledgments

We acknowledge financial support for the project from the Massey University Graduate Research Fund and Geography Department. We also acknowledge field assistance in surveying the ground control points from the Wanganui District Council. We are grateful to

Dr Rob Holman of Oregon State University for useful suggestions and the loan of neutral density filters.

References

1 **R.W.G. Carter.** Man's Response to Sea-Level Change. In R.J.N. Devoy, editor, *Sea Surface Studies: A Global View*, 464-497, Croom Helm, London, 1987.

2 **R.W.G. Carter.** *Coastal Environments.* Academic Press, London, 1988.

3 **E.C.F. Bird.** *Coastline Changes: A Global View.* John Wiley & Sons, London, 1985.

4 **J. Orford.** Coastal Processes: The Coastal Response to Sea-Level Variation. In R.J.N. Devoy, editor, *Sea Surface Studies: A Global View*, 415-451. Croom Helm, London,, 1987.

5 **H.A. Viles.** The Greenhouse Effect, Sea-Level Rise and Coastal Geomorphology. *Progress in Physical Geography*, 13:452-461, 1989.

6 **G. Masselink and A.D. Short.** The Effect of Tide Range on Beach Morphodynamics and Morphology: A Conceptual Beach Model. *Journal of Coastal Research*, in press.

7 **T.C. Lippmann and R.A. Holman.** Quantification of Sand Bar Morphology: A Video Technique Based on Wave Dissipation. *Journal of Geophysical Research*, 94(C1): 995-1011, 1989.

8 **J.L. Davies.** Geographical Variation in Coastal Development. In K.M. Clayton, editor, *Geomorphology Texts 4.* Longman, London, 1980.

9 **R.A. Holman and T.C. Lippmann.** Remote Sensing of Nearshore Bar Systems: Making Morphology Visible. In N.C. Kraus, editor, *Coastal Sediments '87. ASCE*, 929-944, 1987.

10 **R. Shand and D.G. Bailey.** *Environmental and Equipment Limitations of Elevated Terrestrial Imaging* . in preparation.

11 **R.C. Gonzalez and P. Wintz.** *Digital Image Processing.* Addison Wesley, Reading Massachusetts, 1987.